

Anomalous $Zb\bar{b}$ Couplings: From LEP to LHCBin Yan^{1,*} and C.-P. Yuan^{2,†}¹Theoretical Division, Group T-2, MS B283, Los Alamos National Laboratory,
P.O. Box 1663, Los Alamos, New Mexico 87545, USA²Department of Physics and Astronomy, Michigan State University, East Lansing, Michigan 48824, USA (Received 23 January 2021; revised 19 June 2021; accepted 6 July 2021; published 27 July 2021)

The bottom quark forward-backward asymmetry (A_{FB}^b) data at LEP exhibits a long-standing discrepancy with the standard model prediction. We propose a novel method to probe the $Zb\bar{b}$ interactions through $gg \rightarrow Zh$ production at the LHC, which is sensitive to the axial-vector component of the $Zb\bar{b}$ couplings. The apparent degeneracy of the anomalous $Zb\bar{b}$ couplings implied by the LEP precision electroweak measurements seems to be resolved by the current 13 TeV LHC Zh data, which is, however, dominated by the two data points with high transverse momentum of Z boson whose central values are in conflict with the standard model prediction. We also show the potential of the HL-LHC to either verify or exclude the anomalous $Zb\bar{b}$ couplings observed at LEP through measuring the Zh production rate at the HL-LHC, and this conclusion is not sensitive to the possible new physics contribution induced by top quark or Higgs boson anomalous couplings in the loop.

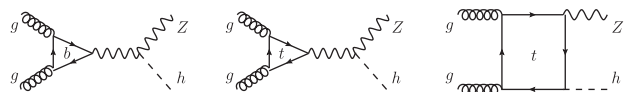
DOI: 10.1103/PhysRevLett.127.051801

Introduction.—The LEP and SLC experiments have measured the Z boson couplings and found most of the electroweak data are consistent with the standard model (SM) predictions with a remarkable precision [1]. However, there are still some experimental results which cannot be explained within the SM framework. A notorious example is that the bottom quark forward-backward asymmetry (A_{FB}^b) measured at the LEP presents a 2.5σ deviation with respect to the SM prediction [1]. As a result, it requires some degree of tuning of the left- and right-handed $Zb\bar{b}$ couplings. One class of intriguing models proposed in the literature to explain the puzzling A_{FB}^b data is to allow a sizable right-handed $Zb\bar{b}$ coupling, while keeping the left-handed $Zb\bar{b}$ coupling about the same as the SM value [2–5]. Although such a large discrepancy in A_{FB}^b could be evidence of new physics (NP) beyond the SM, it is also important to exclude the possibility that it was caused by statistical fluctuation or some subtle systematic errors in experiments. Resolving this puzzle has become one of the core tasks of the next generation lepton colliders, e.g., CEPC, ILC, CLIC, and FCC-ee, which has received much attention by the high energy physics community [6–9]. It has been shown that the $Zb\bar{b}$ anomalous couplings could be well constrained at the future lepton colliders [8].

However, a direct measurement of the $Zb\bar{b}$ couplings at the Large Hadron Collider (LHC) is often ignored in the literature due to the huge backgrounds for detecting the Z boson decaying into a bottom quark and antiquark pair, i.e., $Z \rightarrow b\bar{b}$ or Zb associated production [10,11].

In this Letter, we propose a novel method to probe the $Zb\bar{b}$ couplings through the associated production of Z and the Higgs boson (h) via $gg \rightarrow Zh$ at the LHC. The $Zb\bar{b}$ couplings contribute to the Zh associated production through bottom quark loop effects in the gluon fusion channel, cf. Fig. 1. This process has been widely used to constrain the top quark anomalous couplings, e.g., $Zt\bar{t}$, $ht\bar{t}$, and it has been shown to be sensitive to many NP effects [12–22]. For the first time, we demonstrate that this process can also be used to constrain the bottom quark anomalous couplings and to resolve the A_{FB}^b puzzle.

Owing to charge conjugation invariance, the Z -boson couples only axially to the internal quarks in the loop of diagrams shown in Fig. 1, so that the contribution from a mass-degenerate weak doublet of quarks vanishes. It is worthwhile noting that this conclusion will not be influenced by higher order QCD corrections, because QCD theory preserves vector current conservation due to the symmetry of parity [23–26]. Such a property leads to the

FIG. 1. Illustrative Feynman diagrams of $gg \rightarrow Zh$ production at the LHC.

Published by the American Physical Society under the terms of the Creative Commons Attribution 4.0 International license. Further distribution of this work must maintain attribution to the author(s) and the published article's title, journal citation, and DOI. Funded by SCOAP³.

conclusion that the $gg \rightarrow Zh$ production in the SM would only be sensitive to physics of the third generation quarks, i.e., the bottom and top quarks. Furthermore, as to be shown below, the contribution from the bottom quark is comparable to the top quark in $gg \rightarrow Zh$ production. Therefore, such a process could be used to probe the axial-vector component of the $Zb\bar{b}$ interaction at hadron colliders.

The main difficulty of measuring the $Zb\bar{b}$ couplings at the LHC via the $gg \rightarrow Zh$ process comes from the contamination of the top quark contribution in the loop. One can combine the other measurements at the LHC to constrain the top quark anomalous couplings, e.g., $Zt\bar{t}$ and $ht\bar{t}$ couplings [27–32]. In this Letter, we demonstrate that one could determine the $Zb\bar{b}$ couplings through detecting Zh associated production at the LHC, and the results are not sensitive to the top quark nor the Higgs boson anomalous couplings. Furthermore, we show that the implication of the A_{FB}^b data at LEP can either be verified or excluded if the central value of the signal strength is found to be less than what the SM predicts at the High-Luminosity LHC (HL-LHC), a proton-proton collider to operate at a center-of-mass energy of 14 TeV with an integrated luminosity of 3 ab^{-1} . In that case, our method can also resolve the degeneracy of the $Zb\bar{b}$ couplings, presently allowed by the precision electro-weak data at LEP and SLC.

Zh production via gluon fusion.—We consider the following effective Lagrangian related to Zh associated production,

$$\begin{aligned} \mathcal{L} = & \frac{g_W}{2c_W} \bar{b} \gamma_\mu (\kappa_v^b v_b^{\text{SM}} - \kappa_a^b a_b^{\text{SM}} \gamma_5) b Z_\mu + \frac{m_Z^2}{v} \kappa_Z h Z_\mu Z^\mu \\ & + \frac{g_W}{2c_W} \bar{t} \gamma_\mu (\kappa_v^t v_t^{\text{SM}} - \kappa_a^t a_t^{\text{SM}} \gamma_5) t Z_\mu - \frac{m_t}{v} \kappa_t \bar{t} t h, \end{aligned} \quad (1)$$

where g_W is the weak gauge coupling, c_W is the cosine of the weak mixing angle θ_W , and $v = 246 \text{ GeV}$ is the Higgs vacuum expectation value. The gauge coupling strength modifiers $\kappa_{v,a}^{b,t}$ and $\kappa_{t,Z}$ are introduced to include possible NP effects. The vector and axial-vector couplings of the Z boson to bottom (b) and top (t) quarks in the SM are $v_q^{\text{SM}} = T_3 - 2Qs_W^2$ and $a_q^{\text{SM}} = T_3$, where $(T_3, Q) = (1/2, 2/3)$ and $(-1/2, -1/3)$ for t and b , respectively, with $s_W \equiv \sin \theta_W$. We calculate the helicity amplitudes $M_{\lambda_1, \lambda_2, \lambda_3}$ of the channel $g(\lambda_1)g(\lambda_2) \rightarrow Z(\lambda_3)h$ using FeynArts [33] and FeynCalc [34], where $\lambda_i = +, -, 0$ labels the helicity of particle i . Below, we show the explicit expression of the dominant helicity amplitudes, which can be written, separately for triangle (Δ) and box (\square) diagrams, as

$$\begin{aligned} M_{++0}^\Delta &= 2 \frac{\sqrt{\lambda}}{m_Z} \sum_{t,b} \left\{ \kappa_a^q \kappa_Z \frac{a_q^{\text{SM}} g_{hZZ}}{m_Z^2} [F_\Delta(s, m_q^2) + 2] \right\} N, \\ M_{++0}^\square &= -\frac{4}{m_Z \sqrt{\lambda}} \kappa_a^t \kappa_t g_{ht} a_t^{\text{SM}} m_t [F_{++}^0 + (t \leftrightarrow u)] N, \end{aligned} \quad (2)$$

where

$$\begin{aligned} \lambda &= s^2 + m_Z^4 + m_h^4 - 2(sm_Z^2 + m_Z^2 m_h^2 + m_h^2 s), \\ N &= \frac{\alpha_s g_W}{32\pi c_W}, \end{aligned} \quad (3)$$

and s, t, u are the usual Mandelstam variables for describing the scattering of $gg \rightarrow Zh$. The other couplings are defined as $g_{hZZ} = 2m_Z^2/v$ and $g_{htt} = -m_t/v$. The helicity amplitudes $M_{-0}^{\Delta, \square} = -M_{++0}^{\Delta, \square}$, while the other helicity configurations could be ignored due to their small numerical contributions, about 0.1% at the 14 TeV LHC, to the inclusive production cross section. The definition of the scalar functions F_Δ and F_{++}^0 in Eq. (2) could be found in Ref. [35]. We have compared our analytical results to MADGRAPH5 [36] and found perfect agreement.

Sensitivity at the LHC.—Below, we consider the impact of the nonstandard $Zb\bar{b}$, $Zt\bar{t}$, $ht\bar{t}$, and hZZ couplings to the inclusive cross section of $gg \rightarrow Zh$ at the 14 TeV LHC. In order to compare $\sigma(gg \rightarrow Zh)$ with the SM prediction, we define a ratio $R_{Zh} \equiv \sigma(gg \rightarrow Zh)/\sigma(gg \rightarrow Zh)^{\text{SM}}$. Figure 2 displays the contours of R_{Zh} in the plane of anomalous couplings. The cyan region denotes the constraints from the measurements of the inclusive cross section and transverse momentum distribution of the Z boson (p_T^Z) in the

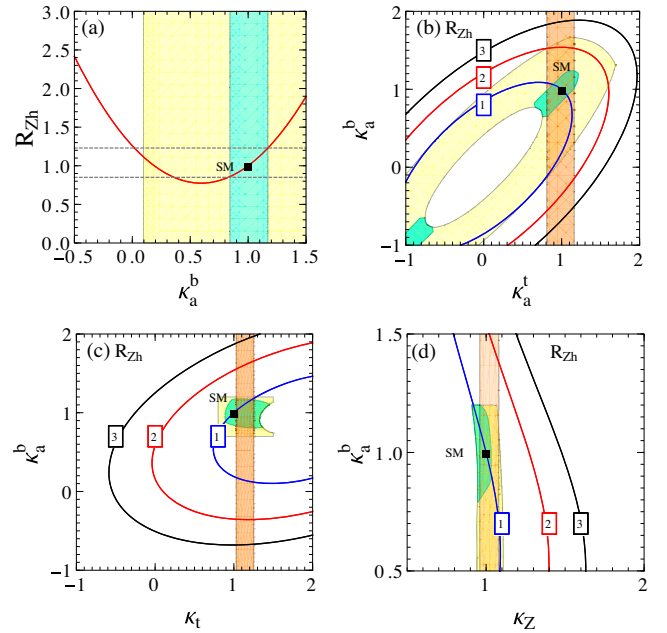


FIG. 2. (a) The contours of R_{Zh} in the plane of anomalous couplings at the 14 TeV LHC. The cyan region denotes the constraints, at 1σ level, provided by the measurements of $pp \rightarrow Zh$ at the 13 TeV LHC, while the yellow shaded region denotes the impact after removing the two high p_T^Z data, depicted in Fig. 4 of Ref. [37]. The orange bands in (b), (c), and (d) come from the constraints of $Zt\bar{t}$, $ht\bar{t}$, and hZZ coupling measurements at the 13 TeV LHC, respectively.

$pp \rightarrow Zh$ production at the 13 TeV LHC [37–41]. The dominant constraint on the parameter space comes from the ATLAS Zh data with high p_T^Z [37], which shows a large deviation from the central value of the signal strength ($\mu_{Zh} \equiv \sigma(pp \rightarrow Zh)/\sigma(pp \rightarrow Zh)^{\text{SM}}$) predicted by the SM, i.e., $\mu_{Zh} = 0.34^{+0.75}_{-0.7}$ and $\mu_{Zh} = 0.28^{+0.97}_{-0.83}$ for $p_T^Z \in [250, 400]$ GeV and $p_T^Z > 400$ GeV, respectively, cf. Fig. 4 of Ref. [37]. If we exclude those two high p_T^Z data points, whose central values happen to be much smaller than the SM predictions, the allowed parameter space is depicted as the yellow band in Fig. 2(a), which shows a much wider uncertainty in κ_a^b as compared to the cyan band (with $0.84 < \kappa_a^b < 1.17$ at 1σ level). Hence, it is important to improve the measurement of the p_T^Z distribution of Zh production at the HL-LHC. The higher order QCD correction effects are taken into account by introducing a constant k factor for both $q\bar{q} \rightarrow Zh$ and $gg \rightarrow Zh$ production processes in the analysis, with $k_{q\bar{q}} = 1.3$ and $k_{gg} = 2.7$ [23,42]. The orange bands in Figs. 2(b)–2(d) show the constraints imposed by the measurements of $Zt\bar{t}$, $h\bar{t}\bar{t}$, and hZZ couplings at the 13 TeV LHC [43–49], respectively. They were obtained by analyzing the production of $Zt\bar{t}$, Ztj , $h\bar{t}\bar{t}$, and $gg \rightarrow h \rightarrow ZZ^*$, etc. The cyan region shown in Fig. 2(b) is constrained by the 13 TeV Zh data while letting both κ_a^t and κ_b^t freely vary within the allowed range imposed by the measurement of $Zt\bar{t}$ couplings. This yields only a slightly larger uncertainty band as $0.66 < \kappa_a^b < 1.23$. Similar analyses, but separately for the anomalous couplings κ_t and κ_Z , are shown in Fig. 2(c) and 2(d). Within the constraints from the current data, the cross section $\sigma(gg \rightarrow Zh)$ could differ from the SM prediction by about 20%–30% (or 100%, if without the inclusion of two above-mentioned high p_T^Z data points) which is a large enough deviation that can be detected at the HL-LHC [50].

At the HL-LHC, many experimental measurements can be further improved as compared to the present data. The error of the signal strengths of Zh and $h\bar{t}\bar{t}$ productions can be reduced to about 4.2% and 4.3%, respectively, while the uncertainty of the branching ratio of $h \rightarrow ZZ^*$ would be at 2.9% [50]. The limit on κ_a^t will also be highly improved through measuring the $t\bar{t}h$, thj , and $gg \rightarrow ZZ$ productions [17,32]. We summarize the expected constraints from the above production processes at the HL-LHC in Figs. 3 and 4. Figure 3 shows that the expected precision for measuring κ_a^b at the HL-LHC is sensitive to the central value of the signal strength μ_{Zh}^0 . Taking $\mu_{Zh}^0 = 0.93$ as an illustration, κ_a^b will be constrained to be $[0.40, 0.78]$ at the 1σ level when we consider κ_a^b alone. As shown in Fig. 1, the Zh associated production cross section also depends on other parameters in Eq. (1). Figure 4 shows the results when we consider only two parameters at a time [50]. The blue band represents the 1σ uncertainty of the Zh associated production cross section measurement with $\mu_{Zh}^0 = 0.93$. In the same figure, the orange shaded regions show the

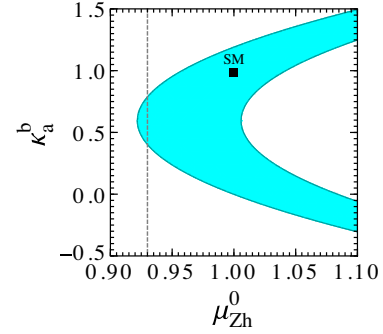


FIG. 3. Expected uncertainty for measuring κ_a^b via Zh associated production at the HL-LHC, as a function of the signal strength μ_{Zh}^0 . The vertical dashed line indicates $\mu_{Zh}^0 = 0.93$.

expected 1σ constraints provided by the $Zt\bar{t}$, $h\bar{t}\bar{t}$, and hZZ coupling measurements at the HL-LHC, respectively. It shows that the HL-LHC measurements of the other processes, such as $Zt\bar{t}$, $h\bar{t}\bar{t}$, and hZZ , will mainly constrain all the anomalous couplings in Eq. (1) except for κ_a^b . Hence, any substantial deviation observed in μ_{Zh} would be ascribed to κ_a^b , whose allowed range will not be noticeably modified by a combined fit with the inclusion of the above-mentioned processes.

Break the $Zb\bar{b}$ coupling degeneracy.—The $Zb\bar{b}$ couplings are also well constrained by the LEP and SLC electroweak data and mainly determined by the Z -pole measurements at the LEP: R_b and A_{FB}^b . The R_b is defined by

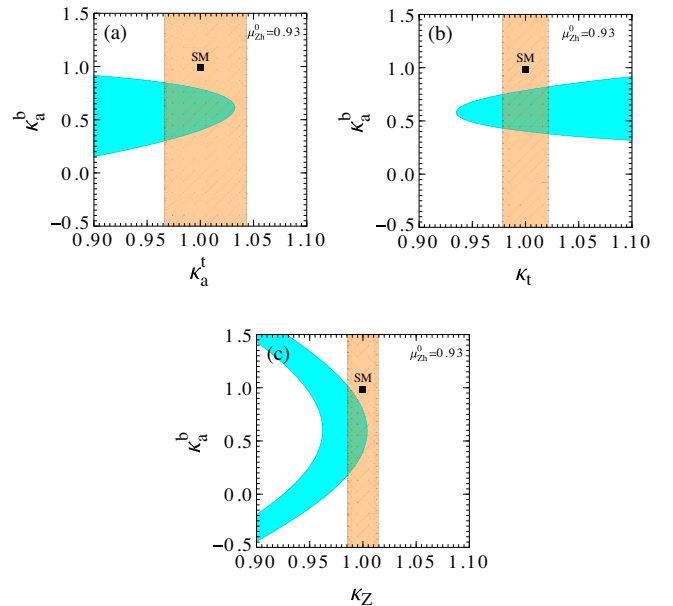


FIG. 4. The blue bands represent the expected uncertainty for measuring κ_a^b via Zh associated production at the HL-LHC. The central value of signal strength is assumed to be $\mu_{Zh}^0 = 0.93$. The orange bands in (a), (b), and (c) represent the expected 1σ constraints provided by the $Zt\bar{t}$, $h\bar{t}\bar{t}$ and hZZ coupling measurements at the HL-LHC, respectively.

the ratio, $R_b = \Gamma(Z \rightarrow b\bar{b}) / \sum_q \Gamma(Z \rightarrow q\bar{q})$, where the sum in the denominator includes all quarks except the top quark. The R_b measurement agrees with the SM prediction very well, while the A_{FB}^b at the Z pole exhibits a large deviation from the SM prediction with a significance around 2.5σ [1,51]. The SLC with a polarized beam can directly probe the bottom quark asymmetry A_b which was found to be consistent with the SM within 1σ [1]. As pointed out in Ref. [2], the Z -pole data alone cannot fully determine the $Zb\bar{b}$ interactions due to the sign ambiguities of the couplings. With the help of A_{FB}^b measurements conducted in the off-shell Z boson region, the part of parameter space with $\kappa_{a,v}^b < 0$ has been excluded. However, it remains to be difficult to resolve the apparent degeneracy in the parameter space with $\kappa_{a,v}^b > 0$ due to the limited statistics for data away from the Z pole. As shown in Fig. 5, both sets of κ_a^b and κ_v^b values, with $(\kappa_a^b, \kappa_v^b) = (1.03, 0.95)$ or $(0.67, 1.46)$, are consistent with the precision electroweak data at LEP and SLC.

To break this degeneracy, one needs to analyze the Zh data collected at LHC. In Fig. 5, we compare the precision on the determination of the axial-vector component of the $Zb\bar{b}$ anomalous coupling via the measurements of inclusive cross section and transverse momentum distribution of Z boson in the Zh production at the 13 TeV LHC to that implied by the precision electroweak data at LEP and SLC. Here, we focus on the parameter space with $\kappa_{a,v}^b > 0$. The cyan and gray shaded regions denote the constraint from R_b and (A_{FB}^b, A_b) measurements with 1σ accuracy, respectively. The orange region in Fig. 5(a) is consistent with the current Zh production measurements, while the orange band in Fig. 5(b) shows the allowed parameter space region after we remove the above-mentioned two high p_T^Z data points [37]. It appears that the current measurement of the Zh inclusive cross section at the LHC has broken the degeneracy in the allowed κ_a^b and κ_v^b values implied by the

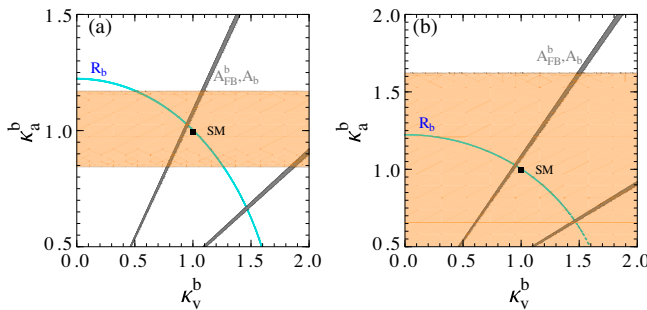


FIG. 5. Present constraints on the axial-vector $Zb\bar{b}$ coupling κ_a^b . The cyan and gray regions come from the R_b , A_{FB}^b , and A_b measurements at LEP and SLC, respectively. The orange band in (a) comes from the measurements of inclusive cross section and p_T^Z distribution of Zh associated production at the 13 TeV LHC, while (b) is the result after removing the two high p_T^Z data in Fig. 4 of Ref. [37].

precision electroweak data, resulting the preferred values of κ_a^b and κ_v^b to be close to 1, the SM values. However, the degeneracy would remain after removing the two high p_T^Z data points whose central values are in conflict with the SM predictions. Hence, it is important to have a more precise measurement of the p_T^Z distribution in the Zh events at the LHC.

Next, we discuss the potential of the HL-LHC to break the above-mentioned degeneracy and determine the value of κ_a^b . The expected constraint on κ_a^b derived from the Zh inclusive cross section measurement at the HL-LHC, assuming an projected uncertainty $\Delta\mu = 4.2\%$ [50], is shown as the orange band in Fig. 6(a), in which the two horizontal lines indicate the two values (1.03 and 0.67) of κ_a^b consistent with the precision electroweak data at LEP and SLC. The degeneracy of κ_a^b (and κ_v^b) found in interpreting the precision electroweak data at LEP and SLC can be broken by the measurement of Zh production cross section at HL-LHC if μ_{Zh}^0 is measured to be less than 0.964 (indicated by the black perpendicular line), which excludes the solution of $\kappa_a^b = 1.03$ allowed by the precision electroweak data and implies new physics beyond the SM must exist (for $\mu_{Zh}^0 \neq 1$). In case that μ_{Zh}^0 is measured to be less than 0.923 (indicated by the purple perpendicular line), the Zh cross section measurement at HL-LHC would exclude the interpretation of the precision electroweak data at LEP and SLC by introducing merely the anomalous κ_a^b and κ_v^b couplings. Moreover, in that case, κ_a^b can be well determined.

On the other hand, when $\mu_{Zh}^0 = 1$, it becomes challenging to test against the A_{FB}^b measurement at LEP by measuring the Zh cross section at HL-LHC, due to the large uncertainty in κ_a^b , cf. Fig. 3. To achieve that goal, a

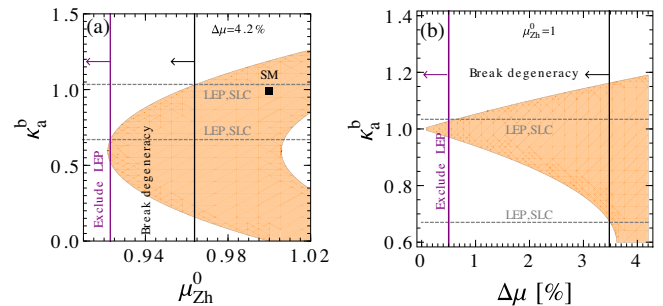


FIG. 6. Expected signal strength μ_{Zh}^0 (a) and precision $\Delta\mu$ (b) for breaking the $Zb\bar{b}$ coupling degeneracy (black perpendicular line) and excluding LEP A_{FB}^b measurement (purple perpendicular line) at the 14 TeV LHC. The two gray (horizontal) dashed lines indicate the degeneracy (at $\kappa_a^b = 1.03$ and 0.67) found in the analysis of LEP and SLC data. The orange band in (a) shows the expected uncertainty on the determination of κ_a^b from measuring the inclusive cross section of the Zh production at the HL-LHC with a fixed $\Delta\mu = 4.2\%$, while (b) is the similar result but with a fixed $\mu_{Zh}^0 = 1$.

much higher precision of the Zh cross section measurement is needed. Figure 6(b) shows the required precision $\Delta\mu$ to break the apparent degeneracy in the $Z\bar{b}b$ couplings, as implied by the LEP and SLC electroweak data, is 3.5% (black perpendicular line). To exclude the interpretation of the A_{FB}^b data at LEP by introducing merely the anomalous κ_a^b and κ_v^b couplings would require $\Delta\mu = 0.5\%$ (indicated by the purple perpendicular line). However, current study on the Zh cross section measurement at HL-LHC [50] projects a 2.6% statistical error, 1.3% experimental systematic error, and 3.1% theoretical uncertainty. Hence, $\Delta\mu = 3.5\%$ might be hopeful to reach at HL-LHC, with an improvement in the theoretical calculation accuracy. But, it would be very challenging to reach $\Delta\mu = 0.5\%$. Nevertheless, measuring the cross section of Zh production can clearly break the apparent degeneracy of the $Z\bar{b}b$ couplings, as implied by the precision electroweak data at LEP and SLC.

Conclusions.—In this Letter, we propose a novel signature to probe the anomalous $Zb\bar{b}$ couplings through measuring the cross section of the Zh associated production via gluon-gluon fusion at the LHC. Our method could be used to break the apparent degeneracy in the $Z\bar{b}b$ couplings, as implied by the LEP and SLC precision electroweak data, including the long-standing discrepancy of the A_{FB}^b data from LEP. We show that the Zh cross section at the one-loop level depends on the axial-vector component of the $Zb\bar{b}$ coupling. The determination of κ_a^b is sensitive to the central value of the signal strength (μ_{Zh}^0) of Zh production, and is not sensitive to possible new physics contribution induced by top quark or Higgs boson anomalous couplings in the loop. The HL-LHC measurements of the other processes, such as $Zt\bar{t}$, $ht\bar{t}$, and hZZ , will mainly constrain all the anomalous couplings in Eq. (1) except for κ_a^b . Hence, any substantial deviation observed in μ_{Zh} would be ascribed to κ_a^b . If μ_{Zh}^0 is found to be noticeably less than 1, the degeneracy of the $Zb\bar{b}$ couplings found interpreting the precision electroweak data at LEP and SLC can be broken and new physics beyond the SM must exist.

This work is partially supported by the U.S. Department of Energy, Office of Science, Office of Nuclear Physics, under Contract No. DE-AC52-06NA25396, [under an Early Career Research Award (C. Lee),] and through the LANL/LDRD Program, as well as the U.S. National Science Foundation under Grant No. PHY-2013791. C.-P. Yuan is also grateful for the support from the Wu-Ki Tung endowed chair in particle physics.

*binyan@lanl.gov

†yuan@pa.msu.edu

[1] S. Schael *et al.* (ALEPH, DELPHI, L3, OPAL, SLD, LEP Electroweak Working Group, SLD Electroweak Group,

SLD Heavy Flavour Group Collaborations), *Phys. Rep.* **427**, 257 (2006).

[2] D. Choudhury, T. M. P. Tait, and C. E. M. Wagner, *Phys. Rev. D* **65**, 053002 (2002).

[3] K. Agashe, R. Contino, L. Da Rold, and A. Pomarol, *Phys. Lett. B* **641**, 62 (2006).

[4] D. Liu, J. Liu, C. E. M. Wagner, and X.-P. Wang, *Phys. Rev. D* **97**, 055021 (2018).

[5] A. Crivellin, C. A. Manzari, M. Alguero, and J. Matias, *Phys. Rev. Lett.* **127**, 011801 (2021).

[6] M. Bicer *et al.* (TLEP Design Study Working Group), *J. High Energy Phys.* **01** (2014) 164.

[7] H. Baer *et al.*, arXiv:1306.6352.

[8] S. Gori, J. Gu, and L.-T. Wang, *J. High Energy Phys.* **04** (2016) 062.

[9] M. Dong *et al.* (CEPC Study Group), arXiv:1811.10545.

[10] M. Beccaria, N. Orlando, G. Panizzo, F. M. Renard, and C. Verzegnassi, *Phys. Lett. B* **713**, 457 (2012).

[11] M. Beccaria, G. Macorini, G. Panizzo, and C. Verzegnassi, *Phys. Lett. B* **730**, 149 (2014).

[12] R. V. Harlander, S. Liebler, and T. Zirke, *J. High Energy Phys.* **02** (2014) 023.

[13] B. Hespel, F. Maltoni, and E. Vryonidou, *J. High Energy Phys.* **06** (2015) 065.

[14] C. Englert, M. McCullough, and M. Spannowsky, *Phys. Rev. D* **89**, 013013 (2014).

[15] L. M. Carpenter, T. Han, K. Hendricks, Z. Qian, and N. Zhou, *Phys. Rev. D* **95**, 053003 (2017).

[16] C. Englert, R. Rosenfeld, M. Spannowsky, and A. Tonero, *Europhys. Lett.* **114**, 31001 (2016).

[17] A. Azatov, C. Grojean, A. Paul, and E. Salvioni, *J. High Energy Phys.* **09** (2016) 123.

[18] D. Goncalves and J. Nakamura, *Phys. Rev. D* **98**, 093005 (2018).

[19] R. Harlander, J. Klappert, C. Pandini, and A. Papaefstathiou, *Eur. Phys. J. C* **78**, 760 (2018).

[20] E. Vryonidou and C. Zhang, *J. High Energy Phys.* **08** (2018) 036.

[21] C. Degrande, F. Maltoni, K. Mimasu, E. Vryonidou, and C. Zhang, *J. High Energy Phys.* **10** (2018) 005.

[22] K.-P. Xie and B. Yan, arXiv:2104.12689.

[23] A. Hasselhuhn, T. Luthe, and M. Steinhauser, *J. High Energy Phys.* **01** (2017) 073.

[24] J. Davies, G. Mishima, and M. Steinhauser, *J. High Energy Phys.* **03** (2021) 034.

[25] L. Chen, G. Heinrich, S. P. Jones, M. Kerner, J. Klappert, and J. Schlenk, *J. High Energy Phys.* **03** (2021) 125.

[26] L. Alasfar, G. Degrande, P. P. Giardino, R. Gröber, and M. Vitti, *J. High Energy Phys.* **05** (2021) 168.

[27] Q.-H. Cao and B. Yan, *Phys. Rev. D* **92**, 094018 (2015).

[28] Q.-H. Cao, S.-L. Chen, and Y. Liu, *Phys. Rev. D* **95**, 053004 (2017).

[29] O. Bessidskaia Bylund, F. Maltoni, I. Tsirikos, E. Vryonidou, and C. Zhang, *J. High Energy Phys.* **05** (2016) 052.

[30] Q.-H. Cao, S.-L. Chen, Y. Liu, R. Zhang, and Y. Zhang, *Phys. Rev. D* **99**, 113003 (2019).

[31] G. Li, L.-X. Xu, B. Yan, and C.-P. Yuan, *Phys. Lett. B* **800**, 135070 (2020).

[32] Q.-H. Cao, B. Yan, C. P. Yuan, and Y. Zhang, *Phys. Rev. D* **102**, 055010 (2020).

- [33] T. Hahn, *Comput. Phys. Commun.* **140**, 418 (2001).
- [34] V. Shtabovenko, R. Mertig, and F. Orellana, *Comput. Phys. Commun.* **207**, 432 (2016).
- [35] B. A. Kniehl and C. P. Palisoc, *Phys. Rev. D* **85**, 075027 (2012).
- [36] J. Alwall, R. Frederix, S. Frixione, V. Hirschi, F. Maltoni, O. Mattelaer, H. S. Shao, T. Stelzer, P. Torrielli, and M. Zaro, *J. High Energy Phys.* **07** (2014) 079.
- [37] G. Aad *et al.* (ATLAS Collaboration), *Phys. Lett. B* **816**, 136204 (2021).
- [38] M. Aaboud *et al.* (ATLAS Collaboration), *Phys. Lett. B* **786**, 59 (2018).
- [39] M. Aaboud *et al.* (ATLAS Collaboration), *J. High Energy Phys.* **05** (2019) 141.
- [40] G. Aad *et al.* (ATLAS Collaboration), *Eur. Phys. J. C* **81**, 178 (2021).
- [41] CMS Collaboration, Report No. CMS-PAS-HIG-19-005, 2020.
- [42] D. de Florian *et al.* (LHC Higgs Cross Section Working Group), [arXiv:1610.07922](https://arxiv.org/abs/1610.07922).
- [43] A. M. Sirunyan *et al.* (CMS Collaboration), *Phys. Rev. Lett.* **122**, 132003 (2019).
- [44] M. Aaboud *et al.* (ATLAS Collaboration), *Phys. Lett. B* **784**, 173 (2018).
- [45] A. M. Sirunyan *et al.* (CMS Collaboration), *Phys. Rev. Lett.* **120**, 231801 (2018).
- [46] A. M. Sirunyan *et al.* (CMS Collaboration), *J. High Energy Phys.* **03** (2020) 056.
- [47] M. Aaboud *et al.* (ATLAS Collaboration), *Phys. Rev. D* **99**, 072009 (2019).
- [48] G. Aad *et al.* (ATLAS Collaboration), *J. High Energy Phys.* **07** (2020) 124.
- [49] G. Aad *et al.* (ATLAS Collaboration), *Eur. Phys. J. C* **80**, 957 (2020).
- [50] M. Cepeda *et al.*, CERN Yellow Rep. Monogr. **7**, 221 (2019).
- [51] M. Baak, J. Cúth, J. Haller, A. Hoecker, R. Kogler, K. Mönig, M. Schott, and J. Stelzer (Gfitter Group), *Eur. Phys. J. C* **74**, 3046 (2014).